High-fidelity Modeling and Optimization of Conjugate Heat Transfer in Arrays of Heated Cables

Zhicheng Wang, George Em Karniadakis
Julie Chalfant, Chryssostomos Chryssostomidis
Massachusetts Institute of Technology, Cambridge, MA
Email: zhicheng@mit.edu

Hessam Babaee
University of Pittsburgh, Pittsburgh, PA

***Abstract*—Following the development of modeling of heat transfer in two-phase flows [1], we have developed a new high-fidelity *conjugate* heat transfer capability that enables the design of effective cooling techniques in multi-solid/multi-fluid systems. We first verified and validated our model with analytical and experimental results. Subsequently, we used the new methodology to study heat transfer around power cables carrying high currents. We first considered an array of cables with staggered arrangement. Our direct numerical simulation (DNS) results demonstrated that the naturally convected flow leads to a strong horizontal traveling wave in between the cable rows. The strength of the traveling wave, however, is strongly non-uniform in different cable rows, resulting in a significant temperature difference of cables at different rows with the temperature of the cable carrying current of $I = 1000$ Amp above $90^{\circ}C$. We then considered a configuration with many more cables (120) but carrying lower current of $I = 80$ Amp. Using different cooling conditions around the box of cables, we found that the maximum temperature never exceeds $50^{\circ}C$. These two different configurations provide possible effective solutions for the design and optimization of the thermal cooling of cables in the 95MW All-Electric-Ship.**

I. Introduction

The thermal design in the All-Electric-Ship (AES) is a major task as thermal loads are tens of MWs and heat fluxes often exceed 100 W/cm^2. The objective of this work is to quantify the temperature field in a two-dimensional array of cylindrical cables carrying very high current densities (12KV and 500 Amps) as well as low current densities subject to both forced and natural convection. Specifically, we aim to optimize the array configuration so that the maximum temperature in the cables is minimized. We are concerned here with conjugate heat transfer as shown in Figure 1, for a two-dimensional array of high-power electric cables. Both natural and forced convection are simultaneously considered as we assume that there is an active forced cooling method in place. For high-power cables, the surface temperature of the cable can potentially exceed the maximum allowable temperature beyond which damage to the insulation layer might occur. For this study, the primary quantity of interest (QoI) is the surface temperature of the cable.

To solve the conjugate heat transfer problem we employ the Smooth Profile Method (SPM) [2], which can be used effectively in complex-geometry flow and heat transfer simulations. In preliminary work in [3] we have extended this method to also deal with conjugate heat transfer and validated it against experimental results. We use a spectral element discretization [4], which allows great flexibility in changing adaptively the resolution as needed. In addition, we can verify the accuracy of the simulation without changing the mesh but by simply increasing the spectral polynomial order per spectral element (p-refinement).

II. Mathematical formulation of conjugate heat transfer

Exact formulation of many convective heat transfer problems requires boundary conditions that consist of *conjugation* of the solid and fluid temperature fields at their interface. The conjugation condition enforces the *balance of energy* at the interface:

$$-k_f \frac{\partial T_f}{\partial \mathbf{n}} = -k_s \frac{\partial T_s}{\partial \mathbf{n}},$$

where the subscript s and f denote solid and fluid, and k and T are the conductivity and temperature of their respective medium. The vector $\mathbf{n}$ is the unit vector normal to the interface. Enforcing the above condition, inherently, requires solving for the temperature field both in the solid and fluid simultaneously, where in the solid medium the thermal field is governed by *conduction*, and in the fluid medium it is governed by *advection-diffusion* process. Absent of enforcing the above condition, one has to resort to assumptions such as isothermal, adiabatic or generally constant-heat-flux walls, if the fluid temperature is the primary Quantity of Interest (QoI). On the other hand, in applications where the solid temperature is the QoI, one has to rely on experimental data or existing correlations to obtain convective the heat transfer coefficient at the wall. Either of these assumptions/limitations could significantly hamper the predictive capability of the models, particularly in cases where strong temperature variation in solid and fluid regions exist. The brute force approach to satisfy the balance of energy in both media is to iterate back and forth between the fluid and solid solvers until temperatures in both media converge. However, the computational cost of the iterations in most three-dimensional applications is significant. Here we present a physics-based model along with a numerical algorithm that: (1) avoids iteration between solid and fluid solvers, and (2) satisfies the balance of energy at the fluid/solid interface and thus does not require *ad-hoc* assumptions at the interface.

Figure 1 shows a schematic of a power cable whose current generates heat inside the cable. For high-current power cables, the surface temperature of the cable can potentially exceed the maximum allowable temperature beyond which melting of the insulation layer might occur. Therefore the primary QoI is the surface temperature of the cable. To find the surface temperature, one has to solve the conduction problem for the cable

$$\rho_s c_s \frac{\partial T}{\partial t} = \nabla \cdot (k_s \nabla T) + q_s(\mathbf{x}, t) \qquad (1)$$
$$-k_s \nabla T.\mathbf{n} = q''_w$$

at the cable/fluid boundary, where ρ is the density, c is the specific heat capacity, and $q''_w := q''_w(\mathbf{x}, t)$ is the local heat flux defined on the surface of the cable, where the subscript w indicates the value at the wall. The heat flux q''_w extracts heat from the cable and is calculated by:

$$q''_w = h(T - T_\infty) \qquad (2)$$

where $h := h(\mathbf{x}, t)$ is the appropriate convective heat transfer coefficient. Due to the complexity of the naturally convected flow around the cable, simple assumptions about the value of h can lead to gross errors in estimating the surface temperature of the cable. To compute h, the convection-driven flow around the cable must be resolved in conjunction with the conduction equation (1).

A. Physics-based modeling

From the physics point of view, for low-power currents, the air surrounding the cable remains stagnant. As a result, the heat extraction from the cable is by pure conduction through the air. For high enough currents, however, the hotter and lighter air surrounding the cable becomes unstable; as the *destabilizing* buoyancy force overcomes the *stabilizing* viscous force, naturally convected flow around the cable is initiated. We use the *Boussinesq approximation* to relate the fluid density to temperature:

$$\rho_\infty - \rho \simeq \rho\beta(T - T_\infty),$$

where the subscript ∞ shows the reference state, and β $(1/K)$ *volumetric thermal expansion coefficient*. Substituting the Boussinesq approximation in the momentum equation results in:

$$\frac{\partial \mathbf{u}}{\partial t} + (\mathbf{u} \cdot \nabla)\mathbf{u} = -\nabla p + \nu_f \nabla^2 \mathbf{u} + \beta(T - T_\infty)\mathbf{g}$$

The temperature in the fluid region is computed by solving the energy equation:

$$\rho_f c_f \Big(\frac{\partial T}{\partial t} + (\mathbf{u} \cdot \nabla)T\Big) = \nabla \cdot (k_f \nabla T) + q_s(\mathbf{x}, t), \qquad (3)$$
$$-k_f \nabla T.\mathbf{n} = q''_w.$$

Coupling heat transport equations models within the solid and fluid regions expressed by equations (1) and (3), along with conservation of mass and momentum in the fluid region results in the following set of coupled partial

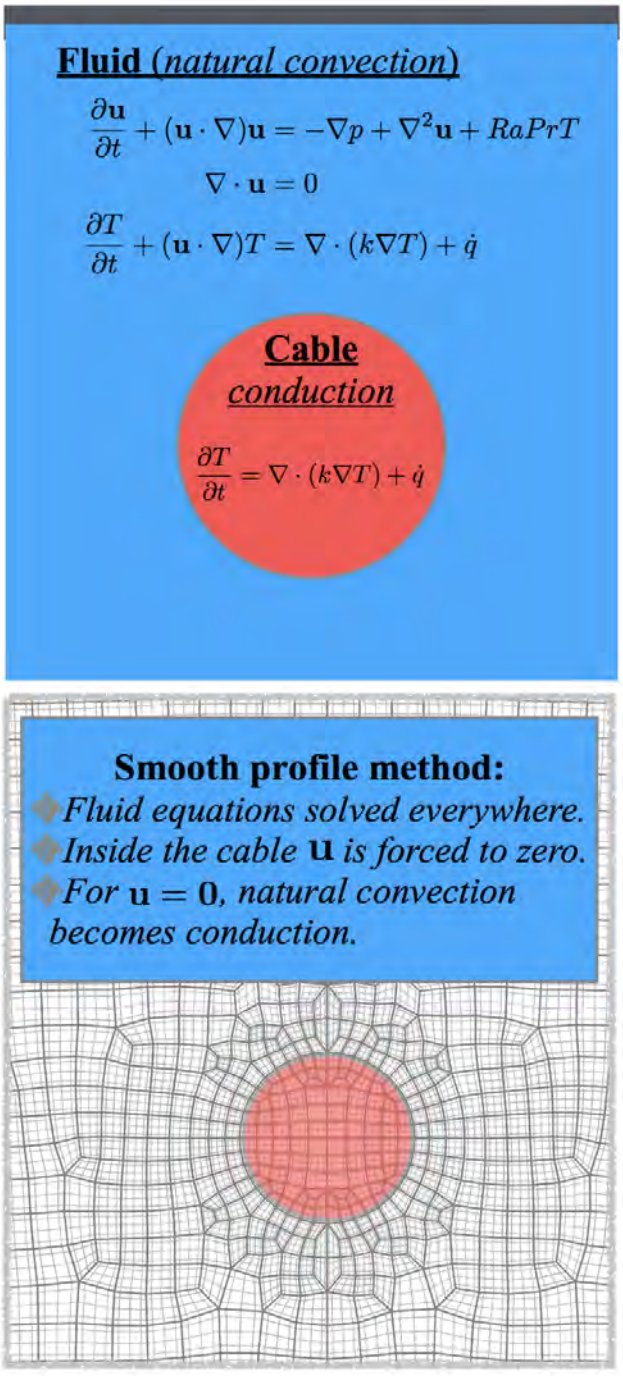

Fig. 1: High-fidelity modeling of conjugate heat transfer around a cable (up) and corresponding spectral element mesh (bottom).

differential equations:

$$\frac{\partial \mathbf{u}}{\partial t} + (\mathbf{u}\cdot\nabla)\mathbf{u} = -\nabla p + \nu_f \nabla^2 \mathbf{u} + \beta(T - T_\infty)\mathbf{g} \tag{4}$$

$$\nabla \cdot \mathbf{u} = 0 \tag{5}$$

$$\rho_f c_f \big(\frac{\partial T}{\partial t} + (\mathbf{u}\cdot\nabla)T\big) = \nabla\cdot(k_f \nabla T) + q_s(\mathbf{x},t) \tag{6}$$

$$\rho_s c_s \frac{\partial T}{\partial t} = \nabla\cdot(k_s \nabla T) + q_s(\mathbf{x},t) \tag{7}$$

$$-k_f \nabla T.\mathbf{n} = -k_s \nabla T.\mathbf{n} \tag{8}$$

where the last equation is valid at the fluid/solid interface. The above equations represent the physics-based model for conjugate heat transfer applications. The presented model could also be utilized in dimension-reduction techniques to create low-dimensional model of the above partial differential equations. The reduced models can then be used in system-level simulation tools and more systematic optimization studies [5], [6].

B. Numerical method

Our discretization is based on Spectral/hp element method implemented in *Nektar*, in which we use spectral polynomials in each element, and time-splitting method to advance the equations in time. The spectral/hp element method has been used in a wide range of applications and more relevantly in highly turbulent forced convection film cooling problems [7], [8]. It is straightforward to show that the fluid/heat transport equations reduce to the conduction equation by setting:

$$\begin{aligned} \mathbf{u} &\to 0 && \text{in solid} \\ c_f &\to c_s && \text{in solid} \\ \rho_f &\to \rho_s && \text{in solid} \\ k_f &\to k_s && \text{in solid} \end{aligned}$$

This embedding of the solid heat transport model in the fluid convection/diffusion equation is exploited in our numerical algorithm by solving the fluid equation everywhere, *i.e.* both in solid and fluid, while using the above conditions in the solid region.

1) Enforcing zero velocity in the solid region: To enforce velocity to zero in the solid region, we employ the Smooth Profile Method [2], in which each solid region is represented by a smooth profile, which equals *unity* in the solid domain, and *zero* in the fluid domain, and varies smoothly across the solid/fluid interface. The most commonly used profile is:

$$\phi_i(\mathbf{x},t) = \frac{1}{2}\left[\tanh\big(\frac{-d_i(\mathbf{x},t)}{\xi_i}\big) + 1\right], \qquad i = 1,2,\ldots,N. \tag{9}$$

where the index i refers to the ith solid region and $d_i(\mathbf{x},t)$ is the *signed* distance to the ith solid region with positive value outside the solid region, *i.e.* the fluid region, and negative value inside the solid region. The value ξ_i is the thickness of the interface; a small number compared to the size of the solid region.

A smoothly spreading *concentration field* is obtained by adding up $\phi_i(\mathbf{x},t)$ of all solid regions:

$$\phi(\mathbf{x},t) = \sum_{i=1}^{N} \phi_i(\mathbf{x},t). \tag{10}$$

For stationary solid regions, it is easy to show that the total velocity field is obtained by:

$$\mathbf{u}(\mathbf{x},t) = (1 - \phi(\mathbf{x},t))\mathbf{u}_f(\mathbf{x},t). \tag{11}$$

It is clear that inside the solid ($\phi = 1$), $\mathbf{u}(\mathbf{x},t) \to \mathbf{0}$, and outside the solid ($\phi = 0$), $\mathbf{u}(\mathbf{x},t) \to \mathbf{u}_f$. Once the above expression for the total velocity is used for the fluid/heat transport equations, a penalty force term $\mathbf{f}_s$ is added to momentum equation as in the following:

$$\frac{\partial \mathbf{u}}{\partial t} + (\mathbf{u}\cdot\nabla)\mathbf{u} = -\nabla p + \nu\nabla^2\mathbf{u} + \beta(T - T_\infty)\mathbf{g} + \mathbf{f}_s \tag{12}$$

in both fluid and solid. where $\mathbf{f}_s \simeq -\frac{1}{\Delta t}\phi\mathbf{u}$. The penalty term goes to zero in the fluid region where $\phi = 0$, and thus the original momentum equation is retrieved, while within the solid region the penalty term enforces $\mathbf{u} \to \mathbf{0}$. For more details of the implementation of this approach into time-splitting spectral/hp element method see references [2], [9].

2) Balance of energy at the fluid/solid interface: To solve equations (4-8), we use the spectral/hp element method in which we seek the solution in the *weak form*. Therefore the balance of energy at the solid/fluid interface, *i.e.* $-k_f \frac{\partial T_f}{\partial \mathbf{n}} = -k_s \frac{\partial T_s}{\partial \mathbf{n}}$ is naturally enforced. For more details see reference [4].

III. Temperature field around power cables

A. Experimental validation

To validate the computational model for a single-fluid application, we considered free (natural) convection flow from a heated horizontal cylinder beneath an adiabatic ceiling. This problem was investigated in an experimental study [10]. In this study a cylinder with diameter D is placed below an adiabatic wall with $L = 2D$ vertical distance from the ceiling to the center of the cylinder. The Rayleigh number $Ra = \frac{g\beta(T_s - T_\infty D^3)}{\nu\alpha} = 15000$, where g is the acceleration due to gravity, T_s temperature at the surface of the cylinder, ν, α and β are the kinematic viscosity, thermal diffusivity and thermal expansion coefficient of the fluid respectively.

Figure 2 shows the comparison of temperature contours with the interferograms obtained from the experiment. A close qualitative agreement is observed between the computation and the experiment. The largest deviation is observed near the ceiling, which is due to inexact enforcement of the experiment of the adiabatic boundary condition at the ceiling. In our numerical study $\frac{\partial T}{\partial \mathbf{n}} = 0$ is enforced at the ceiling wall.

B. Temperature prediction around a staggered array of cables

The schematic of the heat transfer model of power cable is shown in Figure 1 and the staggered configuration is shown in Figure 3. The driver of the flow is the heat

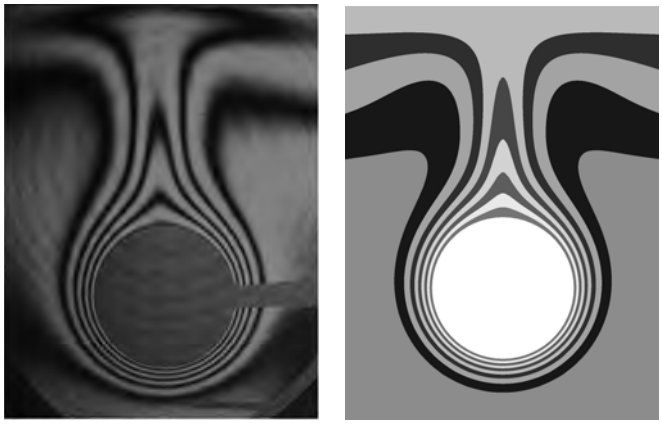

(a) Experiment(taken from [10]) (b) Computation

Fig. 2: Comparison of the computational results with experimental measurements [10] at $Ra = 15000$: (a) interferograms [10], (b) High-fidelity simulations.

generated inside the cable $\dot{Q}$ (W) where $\dot{Q} = \rho l/AI^2$, where ρ_r (Ωm) is the *electrical resistivity*, l (m) is the length of the cable, A (m^2) is the cross-sectional area of the cable, I (Amp) is the current in the cable. For the case considered here the diameter of the cable is $D = 1$ inch, and therefore $A = \pi D^2/4 = 5.07 \times 10^{-4}\ m^2$, the current is $I = 1000$ A, and the electrical resistivity of the copper at 20° C is $\rho_r = 1.68 \times 10^{-8}\ \Omega m$. Therefore, the heat source per unit volume is:

$$\dot{q}_s = \frac{\dot{Q}}{Al} = 65.43 KW/m^3.$$

We use the following non-dimensionalization:

$$t \to \frac{D^2}{\alpha}, \qquad \mathbf{x} \to D, \qquad \mathbf{u} \to \frac{\alpha}{D}, \qquad T - T_\infty \to \frac{D^2 \dot{q}_s}{\alpha \rho c}$$

Therefore, the non-dimensional parameters are:

$$Ra = \frac{\beta D^5 \dot{q} g}{\rho c \nu \alpha^2}, \qquad Pr = \frac{\nu}{\alpha}, \qquad k_r = \frac{k_s}{k_f},$$

where Ra is the Rayleigh number, Pr is the Prandtl number, and k_r is the ratio of the solid conductivity to fluid conductivity. The required air properties at $40°C$ are:

$$\beta = 3.20 \times 10^{-3}(1/K), \quad \nu = 1.70 \times 10^{-5}(m^2/s),$$

$$\alpha = 2.39 \times 10^{-5}(m^2/s), \quad c = 1.00 \times 10^3 (J/KgK).$$

Plugging all of the above properties, the actual Rayleigh number is $Ra = 1.97 \times 10^6$, and Prandtl number is $Pr = 0.71$. At this Ra number the flow is certainly turbulent, and requires high-fidelity DNS to properly resolve the flow and the corresponding thermal boundary layers.

C. Physical insight

In this section, we will report high-fidelity SPM simulations of arrays of cables in staggered arrangement. In

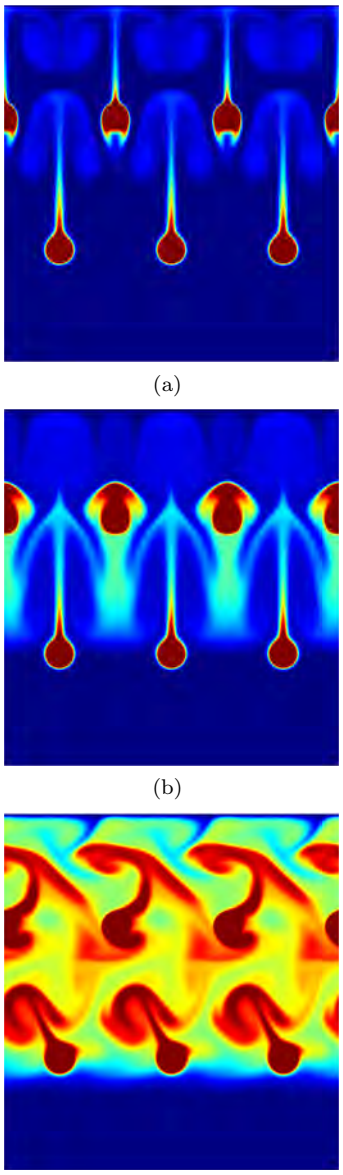

(a)

(b)

(c)

Fig. 3: Snapshots of temperature around heated cylindrical cables. The side boundary conditions are periodic and the bottom and top are isothermal walls. The flow is driven by the heat generated inside the cables. (a): early time; (b): intermediate time; (c): final time.

Figure 3, the evolution of temperature distribution at Ra = 60,000 around the cables is shown. The parameters setup corresponds to a realistic cable setup in the AES. The snapshots show the upward movement of the air. Distinct symmetric vortical structures appear in the beginning of the simulation, however at later times the symmetric pattern breaks down and a traveling wave emerges. These results show that the emerging flow and heat transfer fields are very complex and hence high-fidelity simulations are required to be fused with many lower fidelity simulations to construct a complete stochastic temperature response

surface as a function of the geometry of the array, the Peclet number of the forced convection and the thermal load. This will be done in future work in the context of multi-fidelity simulations as it was demonstrated for a single cylinder subject to mixed (forced/natural) convection in [11]

D. Temperature field around an in-line array of cables

Figure 4 shows the three types of arrangement of cooling devices for 120 electrical cables at $Ra = 16,000$. In Case 1, cooling is applied at the bottom wall; In Case 2, it is applied on the top wall; In Case 3, it is placed on the side walls. Therefore, the corresponding surfaces are treated as isothermal surfaces. The diameter of cables is 1 inch. As shown in Figure 3, the smaller gap spacing among cables is 1 inch, while the larger gap spacing is 2 inch. The current in these cables is 80 Amp. Initially, the temperature is set to be 45^oC. Figure 5 plots the mean and maximum temperature of the three cases. It can be observed that after 15 seconds, the mean temperatures begin to diverge: Case 1 has the highest mean temperature and it keeps growing linearly; Case 2 has the lowest mean value with its growth rate decreasing in time; Case 3 is in between Case 1 and Case 2. On the other hand, the maximum temperatures begin to diverge after 25 seconds and the decay of growth rate of Case 2 is most notable. Figure 6 shows the instantaneous temperature field at 20 seconds of the three cases, where again we observe a very complex temperature filed caused synergistically by natural convection and the complexity in the geometric arrangements.

IV. Conclusion

We have presented a new method for high-fidelity physics-based modeling and a corresponding high-order numerical discretization to study conjugate heat transfer in multi-fluid/multi-solid systems for applications of cooling system design in the All-Electric-Ship (AES). The robustness of the proposed methodology stems from solving a single set of partial differential equations everywhere with varying medium properties in both fluid and solid regions. Its flexibility in treating geometric complex boundaries allowed us for first time to simulate accurately via direct numerical simulation (DNS) an array with 120 cables and assess the effectiveness of various cooling strategies. In particular, we consider two extreme cases, one with a staggered array of a few cables carrying current of 1000 Amp and another one with 120 cables packed in a box in an in-line configuration with each cable carrying current of only 80 Amp. Our simulation results show that in the former case the surface temperature of the cable exceeds $90°C$ while in the latter case the maximum temperature in the system is less than $50°C$. The reason we selected these two extreme cases to study for the thermal performance of the AES is to evaluate the recently proposed designs for different power corridor configurations. In the first design reported in [12] the current was very high, whereas in the most recent design there was a serious effort to lower the value of the bus current. The box with the 120 cables that we considered in our study represents a configuration with

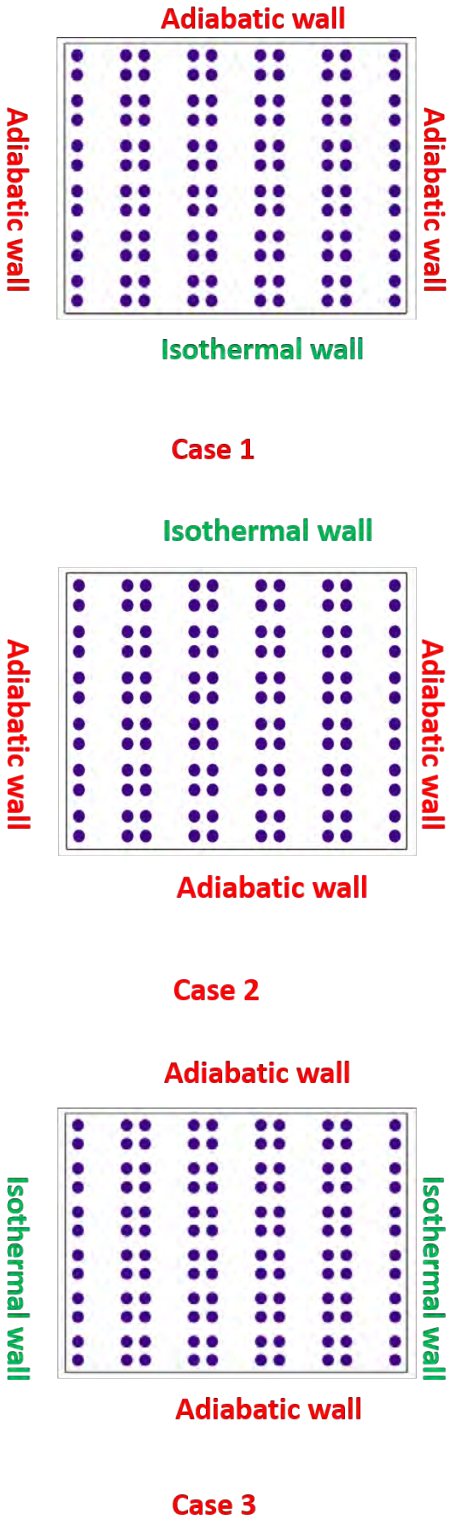

Fig. 4: In-line array of cables: Simulation cases for three different boundary conditions.

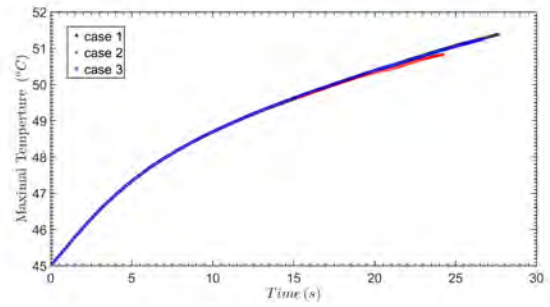

(a)

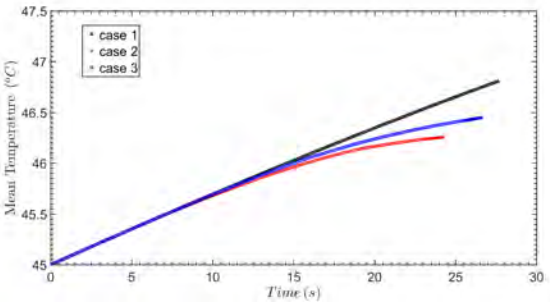

(b)

Fig. 5: Comparison of maximum (a) and mean temperature (b).

more than 17% margin in power carrying capability while the suggested value for the margin is 20%. This means that a new power cable arrangement will require boxes with more than 130 cables to meet that requirement. Clearly, the method we presented here could easily be applied to this new configuration as well.

Acknowledgment

This material is based upon research supported by, or in part by, the U. S. Office of Naval Research (ONR) under award number ONR N00014-14-1-0166 ESRDC âĂŞ Designing and Powering the Future Fleet; ONR N00014-16-1-2956 Electric Ship Research and Development Consortium; N00014-16-1-2945 Incorporating Distributed Systems in Early-Stage Set-Based Design of Navy Ships; and by the National Oceanic and Atmospheric Administration (NOAA) under Grant Number NA14OAR4170077 - MIT Sea Grant College Program.

References

[1] X. Zheng, H. Babaee, S. Dong, C. Chryssostomidis, and G.E. Karniadakis. A phase-field method for 3d simulation of two-phase heat transfer. *International Journal of Heat and Mass Transfer*, 82:282 – 298, 2015.

[2] X. Luo, M. R. Maxey, and G. E. Karniadakis. Smoothed profile method for particulate flows: Error analysis and simulations. *Journal of Computational Physics*, 228(5):1750 – 1769, 2009.

[3] H. Babaee. Conjugate heat transfer with spectral/hp element method. Technical report, MIT Sea Grant Report, 2015.

[4] G. E. Karniadakis and S. J. Sherwin. *Spectral/hp element methods for computational fluid dynamics*. Oxford University Press, USA, 2005.

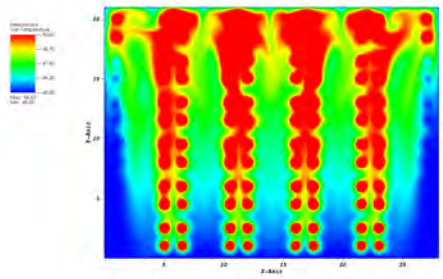

(a) Case 1

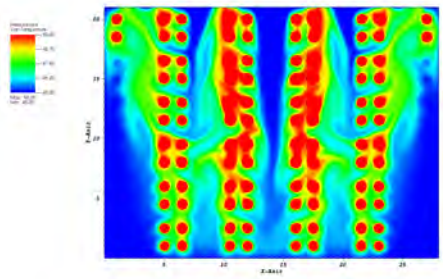

(b) Case 2

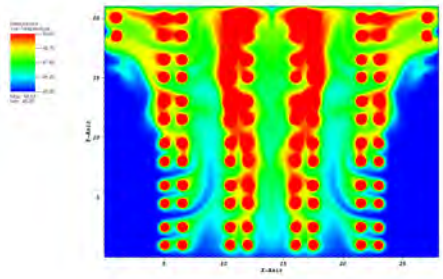

(c) Case 3

Fig. 6: Temperature fields at 20 seconds for the three simulated cases.

[5] H. Babaee, J. Chalfant, C. Chryssostomidis, and A.B. Sanfiorenzo. System-level analysis of chilled water systems aboard naval ships. In *Electric Ship Technologies Symposium (ESTS), 2015 IEEE*, pages 370–375, June 2015.

[6] S. Yang, J.C. Ordonez, J.V.C. Vargas, H. Babaee, J. Chalfant, and C. Chryssostomidis. Comprehensive system-level thermal modeling of all-electric ships: Integration of smcs and vemesrdc. In *Electric Ship Technologies Symposium (ESTS), 2015 IEEE*, pages 251–255, June 2015.

[7] H. Babaee, S. Acharya, and X. Wan. Optimization of forcing parameters of film cooling effectiveness. *Journal of Turbomachinery*, 136(6):061016–061016, 11 2013.

[8] H. Babaee, X. Wan, and S. Acharya. Effect of uncertainty in blowing ratio on film cooling effectiveness. *Journal of Heat Transfer*, 136(3):031701–031701, 11 2013.

[9] X. Luo, A. Beskok, and G. E. Karniadakis. Modeling electrokinetic flows by the smoothed profile method. *Journal of Computational Physics*, 229(10):3828–3847, 5 2010.

[10] M. Ashjaee, A.H. Eshtiaghi, M. Yaghoubi, and T. Yousefi. Experimental investigation on free convection from a horizontal cylinder beneath an adiabatic ceiling. *Experimental Thermal and Fluid Science*, 32(2):614 – 623, 2007.

[11] H. Babaee, P. Perdikaris, C. Chryssostomidid, and G.E. Karniadakis. Multi-fidelity modeling of mixed convection based on experimental correlations and numerical simulations. *Journal of Fluid Mechanics*, 809:895–917, 2016.

[12] C. Chryssostomidis and C. M. Cooke. Space reservation for shipboard electric power distribution systems. In *IEEE Electric Ship technologies Symposium, IEEE ESRS 2015*, pages 187–192, Alexandria, VA, June 2015.